Water Research 169 (2020) 115201

Contents lists available at ScienceDirect

Water Research

journal homepage: www.elsevier.com/locate/watres

Changes in groundwater dissolved organic matter character in a coastal sand aquifer due to rainfall recharge

Liza K. McDonough [a, b, *], Denis M. O'Carroll [a, c], Karina Meredith [d], Martin S. Andersen [a, c], Clément Brügger [a], Hanxue Huang [a, c], Helen Rutlidge [a, c], Megan I. Behnke [e], Robert G.M. Spencer [e], Amy McKenna [f], Christopher E. Marjo [g], Phetdala Oudone [a, b], Andy Baker [a, b]

[a] Connected Waters Initiative Research Centre, UNSW Sydney, NSW, 2052, Australia
[b] School of Biological, Earth and Environmental Sciences, UNSW Sydney, NSW, 2052, Australia
[c] School of Civil and Environmental Engineering, UNSW Sydney, NSW, 2052, Australia
[d] Australian Nuclear Science and Technology Organisation (ANSTO), New Illawarra Rd, Lucas Heights, NSW, 2234, Australia
[e] Department of Earth, Ocean, and Atmospheric Science, Florida State University, Florida, 32310, USA
[f] National High Magnetic Field Laboratory, Florida State University, Tallahassee, FL, 32310-4005, USA
[g] Mark Wainwright Analytical Centre, UNSW Sydney, NSW, 2052, Sydney, Australia

ARTICLE INFO

Article history:
Received 23 August 2019
Received in revised form
14 October 2019
Accepted 15 October 2019
Available online 18 October 2019

Keywords:
FT-ICR MS
LC-OCD
Natural organic matter
Dissolved organic carbon
Coastal aquifer
Sedimentary organic carbon

ABSTRACT

Dissolved organic matter (DOM) in groundwater is fundamentally important with respect to biogeochemical reactions, global carbon cycling, heavy metal transport, water treatability and potability. One source of DOM to groundwater is from the transport of organic matter from the vadose zone by rainfall recharge. Changes in precipitation patterns associated with natural climate variability and climate change are expected to alter the load and character of organic matter released from these areas, which ultimately impacts on groundwater quality and DOM treatability. In order to investigate potential changes in groundwater DOM character after rainfall recharge, we sampled shallow groundwater from a coastal peat-rich sand aquifer in New South Wales, Australia, during an extended period of low precipitation (average daily precipitation rate < 1.6 mm day^{-1} over the 8 months prior to sampling), and after two heavy precipitation events (84 mm day^{-1} and 98 mm day^{-1} respectively). We assess changes in DOM composition after correcting for dilution by a novel combination of two advanced analytical techniques: liquid chromatography organic carbon detection (LC-OCD) and negative-ion electrospray ionization Fourier transform ion cyclotron resonance mass spectrometry (FT-ICR MS). We also assess changes in water chemistry pre- and post-rainfall. Post-rainfall, we show that the dilution-corrected amount of highly aromatic DOM molecular formulae (i.e. those categorised into the groups polyphenolics and condensed aromatics) were 1.7 and 2.0 times higher respectively than in pre-rainfall samples. We attribute this to the flushing of peat-derived DOM from buried organic material into the groundwater. We also identify that periods of low precipitation can lead to low hydrophilic/HOC ratios in groundwater (median = 4.9, n = 14). Redundancy analysis (RDA) was used to compare the HOC fraction with FT-ICR MS compound groups. We show that HOC has a more aromatic character in pre-rainfall samples, and is less similar to the aromatic groups in post-rainfall samples. This suggests that the decline in water-borne hydrophobics observed post-rainfall could be associated with preferential adsorption of the hydrophobic aromatic DOM, making post-rainfall samples less treatable for potable water supply. Post-rainfall we also observe significant increases in arsenic (leading to concentrations greater than 3 times the World Health Organisation drinking water limit of 10 μg / L). Increases in coastal rainfall due to climate change may therefore alter the composition of groundwater DOM in coastal peatland areas in ways that may impact DOM bioavailability, and increase arsenic concentrations, reducing the ease of water treatment for human consumption. To the best of our knowledge, this is the

* Corresponding author. Connected Waters Initiative Research Centre, UNSW Sydney, NSW, 2052, Australia.
E-mail address: l.mcdonough@unsw.edu.au (L.K. McDonough).

https://doi.org/10.1016/j.watres.2019.115201

first study to identify the chemical and molecular changes of shallow groundwater DOM pre-rainfall and post-rainfall in a sedimentary organic carbon rich environment through multiple analytical techniques.

1. Introduction

Half of the global population lives in coastal areas (Post, 2005), with over one billion people relying on coastal aquifers for water supply (Ferguson and Gleeson, 2012; Small and Nicholls, 2003). Recent research has called for the need to identify the impacts of climate change on the quality of freshwater resources (Lipczynska-Kochany, 2018). Dissolved organic matter (DOM), consisting of materials including dissolved organic carbon (DOC), nitrogen and phosphorus, impacts groundwater quality and potability by influencing microbial abundances, driving biogeochemical reactions and assisting the transport of heavy metals (Dalva and Moore, 1991; Harvey et al., 2002; Lalonde et al., 2012). Peatlands, with a total global area of 4.23 million km^2 (Xu et al., 2018), act as a significant store of carbon and source of DOC in groundwater (Rieley et al., 2008; Wang et al., 2018). Climate change is expected to modify these environments, with shifts in precipitation patterns, temperature, and evapotranspiration expected to increase the load of organic matter released from peatlands (Leng et al., 2019; Wasko and Sharma, 2017). Climate change induced rapid sea level rise has also been shown to impact groundwater potability and alter the storage capability of coastal wetlands (Post, 2005; Rogers et al., 2019).

Surface water and shallow groundwater DOC concentrations are often highest in dry seasons due to evapotranspirative concentration, and decline after dilution by low DOC recharge such as snowmelt or precipitation (Dalva and Moore, 1991). However, research has shown that DOC concentration, aromaticity and hydrophobicity in peat environments are highly variable (Broder et al., 2017; Scott et al., 1998; Tang et al., 2013). In sedimentary environments high in organic carbon (OC), heavy rainfall events can cause the flushing of aromatic DOM into groundwater (Broder et al., 2017; Luzius et al., 2018), potentially increasing the load of aromatic DOM drained from these areas. The composition of this DOM may change, with an increase in hydrophilic OC to hydrophobic organic carbon (HOC) ratios in drought conditions previously observed (Scott et al., 1998; Tang et al., 2013) and attributed to the higher solubility of hydrophilic DOM compared to HOC (Scott et al., 1998). This would suggest an increasing difficulty in the treatment of these waters, as hydrophilic molecules have been shown to have lower removal rates during water treatment methods compared to hydrophobic compounds (Jung et al., 2017). This could affect DOM removal efficiency by treatment methods including coagulation (Edzwald, 1993) and ozonation (Peter et al., 2019).

Here, we aim to investigate the impact of extreme wet and dry conditions, on the molecular composition and reactivity of DOM in a high sedimentary OC coastal peatland environment. We compare qualitative molecular-level characterization of DOM isolated before and after major precipitation events in a coastal peatland in Anna Bay, New South Wales (NSW), Australia based on negative-ion electrospray ionization Fourier transform ion cyclotron resonance mass spectrometry (FT-ICR MS). We apply liquid chromatography-organic carbon detection (LC-OCD) to correlate size-based DOM classes and hydrophobicity with elemental compositions derived from FT-ICR MS. Through this combined approach, we propose a mechanism for the observed precipitation-induced DOM compositional shifts. Previous studies have successfully combined size-exclusion chromatography and molecular characterisation techniques to characterise DOM along a soil-stream-river continuum (Hutchins et al., 2017), as well as in marine, riverine and Arctic environments (Bodmer et al., 2016; Chen et al., 2016; He et al., 2016; Retelletti Brogi et al., 2018). Recent research however, indicates that combined method approaches to characterise DOM are still lacking (Derrien et al., 2019). For the first time, this study identifies changes in the concentration and character of hydrophobic and hydrophilic DOM fractions in a groundwater setting after rain following prolonged dry conditions using combined techniques.

2. Materials and methods

2.1. Study site

The research site is located next to a wetland at Samurai Beach in Anna Bay, approximately 150 km north of Sydney, NSW, Australia (Fig. 1). We installed nine multilevel samplers (MLSs) made from PVC tubing (Rakhimbekova et al., 2018) next to the wetland between May and June 2017 using a hand auger. The MLSs are between 1 m and 3 m in length and were installed between 0 and 3 m from the wetland edge (Fig. 1), with sampling ports located at 0.2 m increments down the MLS. MLSA, MLSB, MLSD, MLSE and MLSF are located 1 m apart in a transect oriented east-west. MLSG, MLSH, MLSI, MLSJ were installed between MLA and MLSB and are located 0.2 m apart with slight offsets to the north and south (Fig. 1). The purpose of the MLS installation was to monitor rainfall recharge into the shallow sand aquifer.

Five pre-existing groundwater monitoring bores (S1, S2, S3, S4 and S5) installed in 2011, and a water-level logger installed at the wetland in March 2018 were used to determine groundwater hydraulic gradients and flow directions (Fig. 1, Figure A.1 and Figure A.2).

Samurai Beach sand dunes were formed from Holocene marine and aeolian sands that form well drained, unstable calcareous sand dunes (Bell, 1997), and form part of the Tomaree Sandbeds. The lithology of the aquifer includes sand deposits, peat layers, and a clay unit close to the shoreline (Andersen et al., 2012; Meredith et al., 2019). Water is extracted from the Tomaree Sandbeds in Anna Bay and treated for potable domestic water supply at a water treatment plant located approximately 1.5 km to the north of the study site. Three sources of groundwater have been previously identified to the Tomaree Sandbeds at Samurai Beach through organic and inorganic chemical studies (Brügger, 2018; Meredith et al., 2019). These include water input from wetland, rainwater, and a regional groundwater source. Wetland and rainwater inputs are potentially the most relevant inputs associated with the MLS samples; however it is noted that the wetland was largely dry due to antecedent dry conditions.

The Australian Bureau of Meteorology (BoM) maintains weather stations located at Nelson Bay, New South Wales (NSW) approximately 6.5 km north east of the study site (station number 061054; Lat: 32.71 °S, Long: 152.16 °E) and at Williamtown RAAF, NSW, approximately 26 km west of the study site (station number 061078; Lat: 32.79° S, Long: 151.84° E). Climate data at Nelson Bay

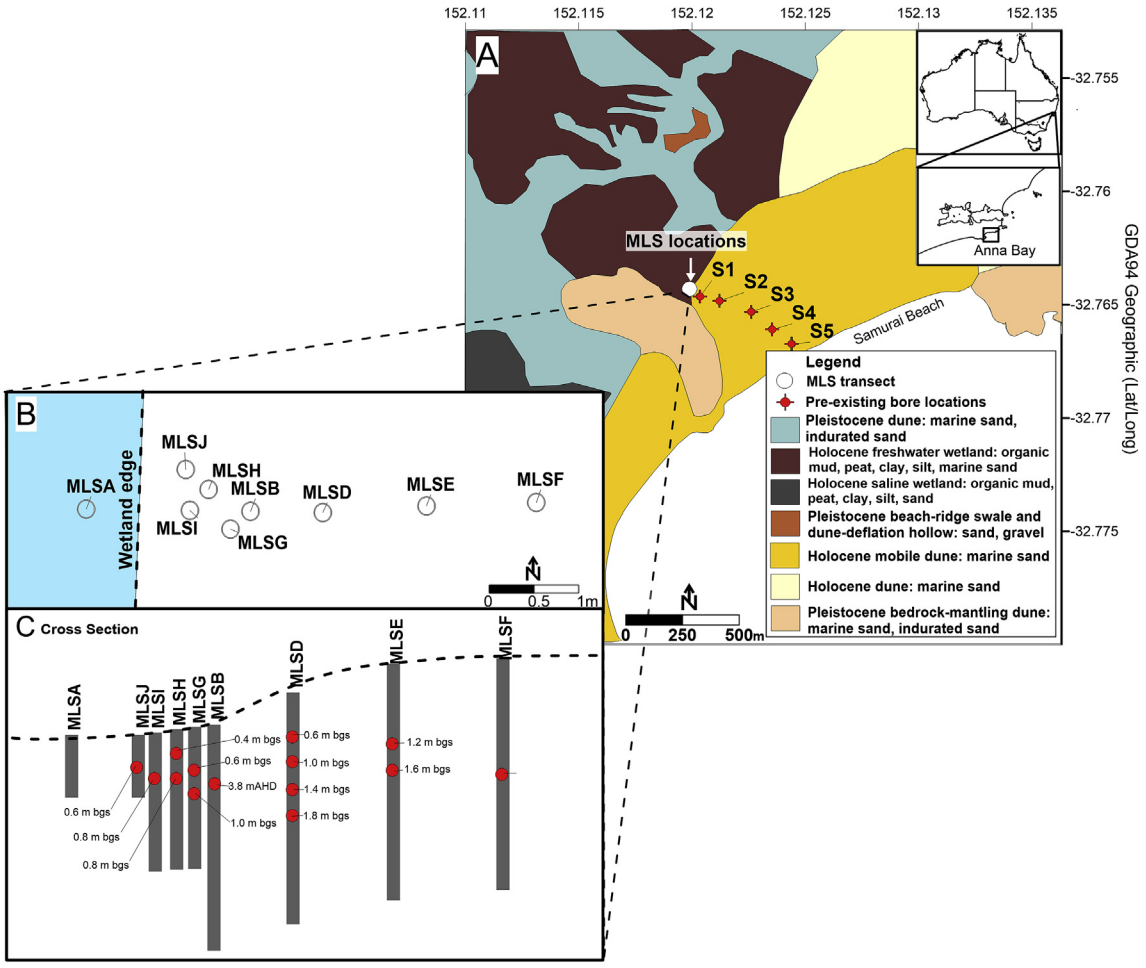

Fig. 1. Sampling locations at Anna Bay, N.S.W., Australia showing A: the local geology, pre-existing well locations and multilevel sampler (MLS) locations, B: zoomed in aerial view of MLS locations, and C: cross section of the MLSs (red circles indicate the 14 MLS ports sampled each trip, with depth shown in meters below ground surface (m bgs)). Figure adapted from Meredith et al. (2019). (For interpretation of the references to colour in this figure legend, the reader is referred to the Web version of this article.)

shows that the area has a warm, temperate climate characterised by high rainfall year-round, with hot summers and mild winters. The long-term average rainfall for Nelson Bay is high at 1345.5 mm / year (1881–2018), with long term high average daily evaporation rates of 11.8 mm in the summer months (December to February) and 2.9 mm in the winter months (June to August, BoM station 061078 between 1974 and 2016).

2.2. Sample collection

Sampling for anions, cations, nitrogen species (nitrate nitrogen ($N-NO_3$) and ammonium nitrogen ($N-NH_4$)), stable water isotopes (^2H and ^{18}O), alkalinity, total DOC, LC-OCD and FT-ICR MS was performed pre-rainfall (February 13, 2018–February 14, 2018) after an uncharacteristically long period of low daily (1.6 mm, $\sigma = 0.7$ mm) rainfall at Nelson Bay between July 2017 and Feb 2018 compared to long term daily averages (4.9 mm, $\sigma = 1.5$ mm) for the same months. Sampling was then performed again after two large rainfall events (March 15, 2018–March 16, 2018 and March 27, 2018–March 28, 2018 where 84 mm and 99 mm of rainfall were recorded respectively). The first sampling campaign was performed at least six months after MLS installation to ensure that sample results were not impacted by any disruption to the natural water-sediment interaction processes caused by installation of the MLSs. Limited water extractability in some MLSs resulted in our sampling of eight of the nine MLSs, with fourteen MLS ports sampled each trip using 50 mL syringes. Less than 500 mL of water was extracted for analysis from each port to minimise the influence on any nearby ports. Samples were filtered in the field using 0.45 μm polyethersulfone filters (Millex).

In-field pH, temperature, electrical conductivity (EC) and dissolved oxygen (DO) were measured using an in-line Sheffield flow-cell attached to two Hach HQ40D multimeters. During the pre-rainfall sampling in February 2018, stable water isotope samples (^2H and ^{18}O) were taken from three locations: MLSA (0.40 m bgs), MLSB (1.00 m bgs) and MLSD (1.15 m bgs). In subsequent trips, stable water isotope samples were sampled from all fourteen ports using 50 mL syringes and filtered using 0.45 μm polyethersulfone filters (Millex). Samples for stable water isotopes were collected in 28 mL McCartney glass bottles with no headspace, and refrigerated at 4 C.

Inorganic anions, nitrogen species ($N-NH_4^+$ and $N-NO_3^-$), total DOC, and LC-OCD (60 mL) samples were collected in 60 mL polyethylene Falcon™ tubes respectively with no headspace, refrigerated, and analysed no later than 7 days after sampling. $^{13}C_{DOC}$ sediment samples were collected at MLSA at depths of 0–10 cm, 10–20 cm and 20–25 cm, and at MLSG at depths of 0–10 cm, 40–50 cm, 90–100 cm, 145–155 cm and 195–205 cm during the pre-rainfall trip, placed in aluminium foil and frozen after sampling to preserve the samples. Samples for cation analysis were collected

in 30 mL acid washed polyethylene vials after filtration, acidified using 65% Suprapur® nitric acid on the day of sampling and refrigerated. Samples for stable isotopes were collected in 28 mL McCartney glass bottles, ensuring no headspace, and refrigerated. FTICR-MS samples were collected in 100 mL HDPE bottles after filtration and frozen. Alkalinity samples were collected in pre-weighed flat bottom 120 mL vials with titration performed using 0.16N sulfuric acid (H_2SO_4) inserted directly into the vials at the end of fieldwork, upon return to the laboratory (maximum 2 days after collection).

2.3. Sample analysis

Anions and cations were analysed at the University of New South Wales (UNSW), Sydney by inductively coupled plasma optical emission spectroscopy (ICP-OES), inductively coupled plasma mass spectrometry (ICP-MS) and ion chromatography (IC). A PerkinElmer Optima 7300 ICP-OES was used to analyse for calcium (Ca), iron (Fe), sodium (Na), potassium (K), magnesium (Mg), sulphur (S), silica (Si) and strontium (Sr), and a PerkinElmer NexION 300D ICP-MS for arsenic (As), aluminium (Al), barium (Ba), phosphorus (P), chromium (Cr), cobalt (Co), copper (Cu), zinc (Zn), nickel (Ni), manganese (Mn) and uranium (U). Chloride (Cl), phosphate (PO_4) and sulphate (SO_4) were analysed by a Dionex IC system with an IonPac AS14A analytical column. Multi-element standards were prepared using single element High-Purity Standards™ at concentrations of 0.2, 1, 10, and 100 mg / L and μg / L. $N{-}NO_3$ and $N{-}NH_4$ were analysed by flow injection analysis at the Mark Wainwright Analytical Centre at UNSW using a Lachat flow injection analyser. Mixed NO_3^- and NH_4^+ standards were prepared fresh for each analysis at concentrations of 0.02, 0.05, 0.20, 0.50, 1.00 and 2.00 mg N / L.

Stable water isotopes (^2H and ^{18}O) were analysed at UNSW by Off-Axis Integrated Cavity Output Spectroscopy using an LGR Liquid Water Isotope Analyser (Lis et al., 2008). VSMOW-2 was used as a primary standard, with an additional five standards used to calibrate samples against. The maximum deviations from the known reference material values were no larger than ±1.0‰ for δ^2H, and ±0.2‰ for $\delta^{18}O$. $\delta^{13}C_{DOC}$ (‰) and percent carbon (C (%)) analysis of sediment was performed using continuous flow isotope ratio mass spectrometry (IRMS) at Australian Nuclear Science Technology Organisation (ANSTO). Dried and crushed sediment samples are introduced into a high temperature elemental analyser (Thermo Fisher Flash 2000 HT EA), combusted into CO_2 at 1020 °C, transferred to a copper reduction furnace at 600 °C where excess O_2 is removed. The gas then passes through a water trap to a Thermo Fisher Conflo IV and into a Thermo Fisher Delta V Plus IRMS. Data are reported relative to International Atomic Energy Agency secondary standards that have been certified relative to the international reference standard Vienna Pee Dee Belemnite. Results are accurate to 1% and ± 0.3‰ for C (%) and $\delta^{13}C_{DOC}$ respectively.

Total DOC concentrations were measured using a total organic carbon (TOC) analyser (Aurora 1030 wet oxidation TOC analyser, OI Analytical, College Station, TX, USA). After acidification and sparging of total inorganic carbon, TOC is measured by chemical oxidation of the OC in the same sample. A DOC-LABOR LC-OCD size-exclusion chromatography system was used to separate classes of dissolved organic materials (organic acids, bases and neutral species). Data processing to identify concentrations of biopolymers (BP, molecular weight > 20,000 g mol^{-1}), humic substances (HS, 500 g mol^{-1} < molecular weight > 10,000 g mol^{-1}), building blocks (BB, 300 g mol^{-1} < molecular weight > 500 g mol^{-1}), low molecular weight acids (LMWA, molecular weight < 350 g mol^{-1}), low molecular weight neutrals (LMWN, molecular weight < 350 g mol^{-1}) and HOC (classified as the material which does not leave the column) was performed using a customised software program (ChromCALC, DOC-LABOR, Karlsruhe, Germany) (Huber et al., 2011). The average difference in DOC concentration obtained by the TOC analyser and by LC-OCD for all samples (n = 42) was 0.51 mg C / L ($\sigma = 0.71$). The linear equation for the comparison of samples analysed by both techniques has a slope of 0.97, an intercept of −0.37 and an R^2 of 0.92. It is important to note that samples high in salt (i.e. those close to seawater concentrations with sodium chloride concentrations of approximately 35 g/L) (Dulaquais et al., 2018) can affect LC-OCD results due to the formation of hypochlorite by UV irradiation which results in the incomplete oxidation of DOC. All samples collected for this study were fresh waters low in sodium (Na, maximum = 28.6 mg / L) and chloride (Cl, maximum = 42.3 mg / L). Size exclusion chromatography has also been shown to result in the fractionation of proteins and polysaccharides in samples (Dulaquais et al., 2018), however proteins represent < 0.5% of DOM in all samples analysed in this study (Table A.2).

DOM molecular character was analysed by FT-ICR MS at the National High Magnetic Field Laboratory in Tallahassee, Florida, USA. Samples for FT-ICR MS analysis were extracted using solid phase extraction onto reversed phase BondElut PPL sorbent (100 mg cartridges, Agilent Technologies) using published methods (Dittmar et al., 2008). Samples were eluted with 1 mL methanol into 2 mL precombusted (550 °C > 5 h) vials and stored frozen until analysis. FT-ICR MS SPE extracts were analysed by negative ion electrospray ionization (Hendrickson et al., 2015; Smith et al., 2018). SPE extract solutions were infused via a microelectrospray source (Emmett et al., 1998) (50 μm i.d. fused silica emitter) at 500 nL / min by a syringe pump at typical conditions for negative ion formation (emitter voltage, −2.2 to -2.9 kV). Ions were accumulated in an external multipole ion guide for 1 − 5 ms and released *m/z* - dependently by a decrease of an auxiliary radio-frequency potential between the multipole roads and the end-cap electrode (Kaiser et al., 2014). Ions were excited to *m/z* - dependent radius to maximize the dynamic range and number of observed mass spectral peaks (*m/z* 150 − 1500, 60% cell radius), and excitation and detection performed on the same pair of electrodes (Chen et al., 2014). The dynamically harmonized ICR cell is operated with 6 V trapping potential (Boldin and Nikolaev, 2011; Hendrickson et al., 2015). 100 time - domain transients of 3.1 s were averaged for all experiments, and mass spectra were internally calibrated with ~5 highly abundant O_x series based on the "walking" calibration method (Savory et al., 2011). Peaks with signal magnitude greater than 6 times the baseline root-mean-square (rms) noise at *m/z* 400 were exported to peak lists, and molecular formula assignments performed with PetroOrg © software (Corilo, 2015). Molecular formula assignment constraints were $C_{1-45}H_{1-92}N_{0-4}O_{1-25}S_{0-2}$. A modified aromaticity index (AI_{mod}) was calculated to assess the degree of unsaturation based on neutral molecular formula (Koch and Dittmar 2006; Koch et al., 2007). Molecular formulae identified by FT-ICR MS may also occur in other isomeric arrangements, however since the molecules assigned to FT-ICR MS peaks describe the underlying molecular compounds of DOM, the term compound is used when discussing these peaks. These compound groups are therefore based on elemental compositions and are not based on compound structural motifs. Compound groups were classified based on AI_{mod} and elemental stoichiometries as follows: polyphenolic ($0.5 < AI_{mod} \leq 0.66$) condensed or polycyclic aromatic ($AI_{mod} > 0.66$); highly unsaturated and phenolic ($AI_{mod} \leq 0.5$, $H/C < 1.5$, $O/C \leq 0.9$); aliphatic ($1.5 \leq H/C \leq 2.0$, $O/C \leq 0.9$ and $N = 0$); sugar-like ($O/C > 0.9$); and peptide-like ($1.5 \leq H/C \leq 2.0$, and $N > 0$).

2.4. Data analysis and statistics

Wilcoxon rank sum tests were used to determine differences between the medians in pre- and post-rainfall data. As zero values were present in the HOC data, 0.05 was added to the HOC concentration before log transforming the data prior to linear model generation to assess the relationship between HOC and other variables. Residuals versus fitted plots and normal Q-Q plots were checked to ensure constant variance and normality assumptions were met after transformation. All statistical analyses and figures were generated using RStudio (v.1.1.456). RDA was performed using the methods provided in Hutchins et al. (2017).

Corrections for the rainfall recharge dilution were performed by averaging the post-rainfall chloride concentrations for each sampling port and dividing the post-rainfall concentrations by pre-rainfall concentrations. The pre-rainfall DOM concentrations were then multiplied by the fraction of chloride remaining in the sample for each port. Any increase or decrease in concentrations of water chemistry parameters or DOM fractions or groups over the values expected due to dilution are reported in the results.

3. Results and interpretation

3.1. Geology and hydrogeology

During MLS installation it was noted that there was an organic rich peat layer at approximately 0.2 m below ground surface (bgs) at MLSA on the wetland edge. This organic rich layer increased in depth with distance from the wetland suggesting buried peat layers in the area. During the MLS installation, clusters of organic material were observed intermittently through the sand. The OC content in these regions was up to 48.5% ± 1 compared to sandy regions which were as low as 0.1% ± 1 OC. The $\delta^{13}C_{DOC}$ (‰) values of the low OC (< 10%) sandy sediment was as high as −7.3‰ whilst the maximum $\delta^{13}C_{DOC}$ (‰) values of the high OC (> 10%) sediment was − 28.2‰ (Table A.1).

The hydraulic gradient between the wetland and S1 is variable with a predominant long-term average gradient and groundwater flow direction from the wetland to the dunes. The average hydraulic conductivity of the upper sandy aquifer has previously been measured using a Hydraulic Profiling Tool (HPT) inserted using a Geoprobe (7822 DT) drill-rig to approximately 16 m/day (Andersen et al., 2012; Brügger, 2018). Using this value and the monitoring of absolute groundwater levels in S1 (lat: -32.76°, long: 152.12°) and in the wetland (lat: -32.76°, long: 152.12°), the average Darcy velocity during the period of sampling was calculated as −0.031 m/day. The negative velocity indicates a reversal in flow from the long-term average to a flow direction running from the dunes to the wetland.

Assuming an effective porosity of 0.3, the water flowed a lateral distance of 1.3 m from the dunes to the wetland between the date of wetland water logger installation (March 15, 2018) and the final sampling trip (March 28, 2018). This indicates that groundwater travelled almost half of the total distance of the MLS transect in one week during sampling. Pre-rainfall samples therefore comprised a mix of water from both the dunes and the wetland, with post-rainfall samples comprising a mix of water originating from the dunes, wetland and rainfall recharge.

The change in water level at well S1 pre- and post-rainfall events was used to estimate the approximate volume of rainfall recharging the aquifer. Post-rainfall, water levels at S1 rose approximately 0.25 m during the heavy precipitation events on the 26th February, 2018 and 22nd March, 2018 (84 mm and 99 mm of rainfall respectively). This indicates that approximately 41% of the total rain volume recharged the aquifer and mixed with groundwater from the wetland and dunes (Brügger, 2018). This is supported by stable water isotopes (Figure A.3, Table A.1), which show that pre-rainfall samples are more enriched ($\delta^{18}O$ average = −2.88 ± 0.11 (1 σ), $\delta^{2}H$ average = −10.17 ± 0.76 (1 σ), n = 3) than post-rainfall ($\delta^{18}O$ average = −3.33 ± 0.54 (1 σ), $\delta^{2}H$ average = −14.70 ± 2.33 (1 σ), n = 24). These values indicate that precipitation events have resulted in fluxes of water that has previously experienced partial evaporation on or close to the surface.

3.2. Groundwater chemistry

The results show that there is a significant decline in the median (non-dilution corrected) concentration of Cl ($p = 2.35 \times 10^{-3}$), Zn ($p = 1.82 \times 10^{-2}$), Mn ($p = 2.97 \times 10^{-2}$), EC ($p = 1.26 \times 10^{-2}$), K ($p = 3.73 \times 10^{-5}$) and Na ($p = 5.22 \times 10^{-4}$) in the post-rainfall samples compared to pre-rainfall samples (Table 1) which can largely be attributed to the input of fresh rainfall recharge. We note an increase in median As ($p = 4.72 \times 10^{-5}$) and a $N{-}NH_4$ ($p = 1.73 \times 10^{-2}$) concentrations post-rainfall (Table 1). Pre-rainfall data reveals a significant negative correlation between HOC and As concentrations ($p = 2.02 \times 10^{-2}$) which is not observed post-rainfall. This has important implications for water treatment and interpretation of these findings are explored in further detail in Section 5. The increase in $N{-}NH_4$ is positively correlated with DOC concentration ($p = 3.32 \times 10^{-2}$ and $p = 1.51 \times 10^{-2}$ pre and post-rainfall respectively) suggesting that the increase in $N{-}NH_4$ post-rainfall may be associated with desorption from DOM or aquifer minerals (Maier, 2015). Changes in the median values of Co, U, $N{-}NO_3$, PO_4 and SO_4 post-rainfall were not assessed as both the pre- and post-rainfall median concentrations were below the limit of detection (LOD, lowest concentration of a substance that can be reliably reported using a specific laboratory method and instrument). There were no significant increases in pre- and post-rainfall in other ions (Table 1) when not corrected for dilution.

Average Cl concentrations in the pre-rainfall samples are 38.01 ± 2.83 mg / L (1 σ). The change in average Cl concentrations at each sampling port from pre-rainfall to post-rainfall ranged from between 0.15% and - 58.00% (average - 26.96 ± 10.31% (95% CI)) with a significant median decline of −29.5% ($p = 2.53 \times 10^{-3}$) as noted above. We assume here that Cl does not undergo any geochemical reactions in the aquifer, since the groundwater is fresh. As Cl is present in very low concentrations (0–2 mg / L) in rainwater (Thomas et al., 2007), the change in Cl concentrations at each port between pre- and post-rainfall sampling trips were used to quantify the extent of dilution expected for water chemistry parameters (Table 1) and concentrations of LC-OCD fractions and FT-ICR MS groups at each sampling port caused by rainfall recharge (Table 2).

After correction for dilution, concentrations of $N{-}NH_4$, P, As, Ca, Mg, Si, Sr, and Ni are shown to significantly increase post-rainfall (Table 1). We suggest that these increases in $N{-}NH_4$, P and As may be a result of desorption from sedimentary organic matter or aquifer minerals (Guppy et al., 2005; Bauer and Blodau, 2006; Maier, 2015). There also appears to be dissolution of carbonate derived elements as evidenced by the increase in Ca, Mg, Si, and Sr post-rainfall after correcting for dilution (Table 1). An increase in Ni is observed after dilution correction however we do not identify any correlation between Ni and hydrophobicity or DOC concentration ($p > 0.05$). We do not observe increases in any other NOM-related metals including Co, Cr, or Cu, and all occur at low median concentrations in pre- and post-rainfall data (< 0.4 μg / L, Table 1).

3.3. Dilution-corrected change in DOM variables

The predicted median post-rainfall DOC concentration (using

Table 1
Median pre-rainfall and post-rainfall concentrations for selected water chemistry parameters (not corrected for dilution) and median concentration expected after dilution (dilution corrected). P-values represent Wilcoxon rank sum test significance of the difference between the median pre-rainfall values and median post-rainfall values averaged over the two trips with no correction for dilution (column 5) and correction for dilution (column 8). Variables with significant differences at the $p = 0.05$ level are shown in bold. Where lab reported values for a sample fell below the limit of detection (LOD), a zero value was used. Where both pre- and post-rainfall medians were below the LOD, p-values were not assessed.

Water chemistry parameter	Median concentration pre-rainfall	Median concentration post-rainfall (not corrected for dilution)	Increase / decrease after rainfall	p-value for change in median concentration (not corrected for dilution)	Median concentration expected after rainfall (dilution corrected)	Increase / decrease after rainfall (dilution corrected)	p-value for change in median concentration (dilution corrected)
EC (µS / cm)	629.5	486.5	Decrease	**1.26×10^{-2}**	458.3		2.27×10^{-1}
PO_4 (mg / L)	< 0.3	< 0.3		NA	< 0.3		NA
SO_4 (mg / L)	< 0.3	< 0.3		NA	< 0.3		NA
$N{-}NH_4$ (mg / L)	< 0.05	0.06	Increase	**1.73×10^{-2}**	< 0.05	Increase	**6.33×10^{-3}**
$N{-}NO_3$ (mg / L)	< 0.05	< 0.05		NA	< 0.05		NA
Na (mg / L)	24.73	14.36	Decrease	**5.22×10^{-4}**	15.94		5.11×10^{-1}
Mg (mg / L)	2.98	3.63		7.09×10^{-1}	2.31	Increase	**4.44×10^{-2}**
Al (µg / L)	11.78	11.48		3.71×10^{-1}	9.03		1.78×10^{-1}
Si (mg / L)	2.42	2.18		2.68×10^{-1}	1.71	Increase	**3.65×10^{-2}**
P (µg / L)	343.08	309.72		5.48×10^{-1}	194.07	Increase	**1.06×10^{-2}**
S (mg / L)	0.57	0.6		8.73×10^{-1}	0.49		1.94×10^{-1}
Cl (mg / L)	38.39	26.18	Decrease	**2.35×10^{-3}**	NA		NA
K (mg / L)	1.23	0.53	Decrease	**3.73×10^{-5}**	0.88		1.37×10^{-1}
Ca (mg / L)	98.38	85.55		2.46×10^{-1}	69.48	Increase	**9.15×10^{-3}**
Cr (µg / L)	0.33	0.35		8.94×10^{-1}	0.29		6.20×10^{-2}
Mn (µg / L)	27.86	17.93	Decrease	**2.97×10^{-2}**	18.32		8.04×10^{-1}
Fe (mg / L)	4.08	3.52		3.71×10^{-1}	2.68		3.76×10^{-1}
Co (µg / L)	< 0.20	< 0.20		NA	< 0.20		NA
Ni (µg / L)	0.3	0.36		3.70×10^{-1}	0.19	Increase	**4.06×10^{-2}**
Cu (µg / L)	0.45	0.86		9.36×10^{-1}	0.35		5.08×10^{-2}
Zn (µg / L)	15.75	12.59	Decrease	**1.82×10^{-2}**	12.1		1.00
As (µg / L)	16.25	34.43	Increase	**4.72×10^{-5}**	12.16	Increase	**3.49×10^{-7}**
Sr (mg / L)	0.81	0.72		2.62×10^{-1}	0.57	Increase	**1.23×10^{-2}**
Ba (µg / L)	9.87	6.5		1.04×10^{-1}	7.91		8.74×10^{-1}
U (µg / L)	< 0.20	< 0.20		NA	< 0.20		NA

Table 2
Median pre-rainfall, predicted post-rainfall and actual post-rainfall LC-OCD fraction (biopolymers (BP), humic substances (HS), building blocks (BB), low molecular weight neutrals (LMWN), hydrophilic organic carbon (CDOC; the sum of BP, HS, BB, and LMWN) and hydrophobic organic carbon (HOC; total DOC minus the CDOC)) concentrations in micrograms per litre (µg / L) and FT-ICR MS group number of formulae. Predicted post-rainfall median values are pre-rainfall values corrected for dilution (calculated by the change in Cl concentrations). P-values represent Wilcoxon rank sum test significance of the difference between the expected median post-rainfall values and actual post-rainfall values. Variables with significant differences at the $p = 0.05$ level are shown in bold.

		Median pre-rainfall	Median post-rainfall predicted by dilution	Actual median post-rainfall	p-value
Total DOC (mg / L)		6.97	4.46	3.85	4.01×10^{-1}
LC-OCD (µg / L)	BP	12.5	7.4	45.5	**3.52×10^{-3}**
	HS	3825.5	2505.2	1613.5	9.39×10^{-2}
	BB	1100.0	640.7	415.8	1.25×10^{-1}
	LMWN	853.0	594.4	591.3	6.67×10^{-1}
	CDOC (hydrophilic)	5977.5	3839.1	2684.0	1.78×10^{-1}
	HOC (hydrophobic)	1172.0	788.1	79.8	**1.01×10^{-4}**
FT-ICR MS (number of formulae)	Sugars	41	27	31	7.69×10^{-1}
	Highly Unsaturated and Phenolic	5907	4405	4890	**3.10×10^{-2}**
	Polyphenolic	1242	771	1348	**2.61×10^{-5}**
	Condensed Aromatics	363	232	473	**4.53×10^{-5}**
	Peptide-like	25	14	3	5.18×10^{-1}
	Aliphatic	526	367	292	6.35×10^{-1}

the change in Cl as a correction factor) was 4.6 mg / L, similar to the observed median concentration (Table 2). The range of minimum and maximum DOC concentration values increased from 5.8 mg / L pre-rainfall (min = 4.79 mg / L, max = 10.55 mg / L) to 8.1 mg / L post-rainfall (min = 1.51 mg / L, max = 9.79 mg / L). Standard deviation increased from 1.8 mg / L to 2.2 mg / L suggesting some MLS ports are more affected by dilution than others. HOC is the only LC-OCD fraction significantly lower in post-rainfall concentrations after correction for dilution ($p = 1.01 \times 10^{-4}$, Table 2). The ionization process and high-resolution of FT-ICR MS produces molecular ions from all species in the sample that can be assigned a molecular formula within specific chemical classes, and peak intensity enables semi-quantitation of these classes. Here, we observe a significant increase in the median number of polyphenolics ($p = 2.61 \times$

10^{-5}), condensed aromatics ($p = 4.53 \times 10^{-5}$) and highly unsaturated and phenolics ($p = 3.10 \times 10^{-2}$) compared to predicted levels after correction for dilution (Table 2).

3.4. LC-OCD fractions and FT-ICR MS compound group relative abundances

In pre-rainfall LC-OCD samples, the HS fraction comprised the largest LC-OCD fraction of DOM, followed by HOC (Fig. 2). Post-rainfall, HS remained the largest LC-OCD fraction, however HOC became the least abundant after BP (Fig. 2). We attribute increases in percent relative abundance (% RA) of HS, BP and LMWN largely to the decrease in % RA HOC. We observe a significant decline in both concentration and % RA of HOC after rainfall recharge, from a median concentration of 1,172.0 μg / L to 79.8 μg / L ($p = 1.01 \times 10^{-4}$) and a median % RA decline from 17.0% to 1.1% ($p = 1.176 \times 10^{-6}$).

For both pre- and post-rainfall recharge, the largest proportion of FT-ICR MS formulae were identified as belonging to the highly unsaturated and phenolic group, followed by the polyphenolic group (Fig. 2). There was a significant increase in the % RA and number of formulae of condensed aromatics ($p = 1.06 \times 10^{-3}$ and $p = 4.49 \times 10^{-3}$ respectively) and polyphenolics ($p = 1.20 \times 10^{-4}$ and $p = 1.19 \times 10^{-3}$ respectively). The median % RA of aliphatics significantly declined ($p = 1.13 \times 10^{-2}$) however the number of aliphatic formulae did not significantly decline ($p = 4.99 \times 10^{-2}$, Table 2) suggesting the decline in % RA is due to the increase in % RA of condensed aromatics and polyphenolics.

3.5. Changes in DOM molecular properties

Weighted median H/C organic matter elemental ratios declined significantly post-rainfall ($p = 2.31 \times 10^{-4}$, Fig. 3) whilst median O/C ratios increased significantly ($p = 2.00 \times 10^{-03}$, Fig. 3). Post-rainfall, median weighted nominal oxidation state of carbon (NOSC) also increased from 0.06 to 0.16 ($p = 5.41 \times 10^{-4}$). Post-rainfall median weighted double bond equivalents (DBE) increased from 11.09 to 11.91 ($p = 4.81 \times 10^{-4}$), median weighted AI_{mod} increased from 0.35 to 0.39 ($p = 1.79 \times 10^{-4}$) and median weighted mass of the samples increases from 474.96 to 481.44 ($p = 4.76 \times 10^{-3}$, Fig. 3). These changes indicate that DOM became larger and more aromatic in character after rainfall recharge.

3.6. Changes in HOC

LC-OCD data shows significant changes in the HOC and BP fractions (Table 2). This assessment however focuses on the changes in HOC as the BP fraction represents < 2% of the total DOM composition. Pre-rainfall, HOC is positively correlated with NOSC and O/C ratios ($p = 2.23 \times 10^{-2}$ and $p = 1.63 \times 10^{-2}$) and negatively correlated with numbers of FT-ICR MS formulae identified ($p = 2.67 \times 10^{-3}$). Post-rainfall HOC is negatively correlated with NOSC ($p = 2.26 \times 10^{-3}$, AI_{mod} ($p = 3.83 \times 10^{-3}$), DBE ($p = 3.30 \times 10^{-3}$) and mass ($p = 8.26 \times 10^{-3}$).

Redundancy analysis (RDA) can be used to explain one dataset using another dataset. In this analysis we compare LC-OCD fractions with FT-ICR MS groups and specifically look at changes in HOC. The RDA results show that HOC in the shallow aquifer at Anna Bay is associated with different molecular groups pre-rainfall recharge compared to post-rainfall. Pre-rainfall, the RDA shows that HOC is most closely associated with condensed aromatics and polyphenolics (Fig. 4, Table A.2). This is also supported by a significant positive relationship between HOC % RA and polyphenolics % RA ($p = 4.99 \times 10^{-3}$) and condensed aromatics % RA ($p = 1.12 \times 10^{-2}$). Pre-rainfall there is also a significant negative relationship between HOC % RA and highly unsaturated and phenolics % RA ($p = 1.21 \times 10^{-2}$) and aliphatics % RA ($p = 2.48 \times 10^{-4}$). Interestingly, the redundancy analysis (Fig. 4B, Table A.2) shows HOC is most strongly correlated with these two FT-ICR MS groups, and least correlated with condensed aromatics and polyphenolics post-rainfall. These observations are also reflected in simple linear

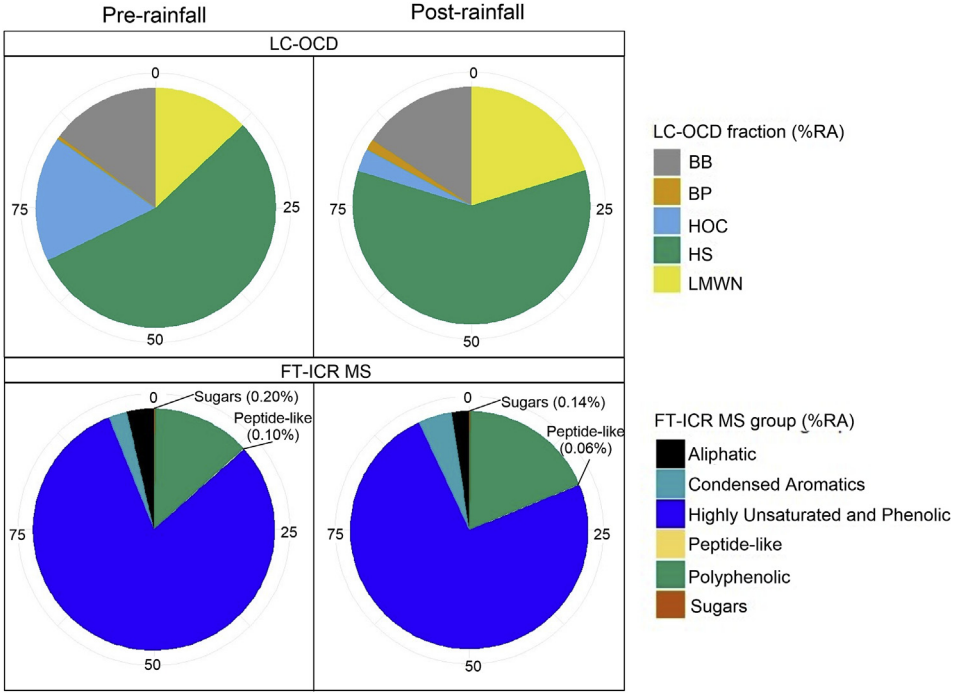

Fig. 2. Pie charts showing average percent relative abundances (% RA) of LC-OCD fractions (upper charts) and FT-ICR MS groups (lower charts) in samples for pre-rainfall (n = 14) and post-rainfall (n = 28) samples.

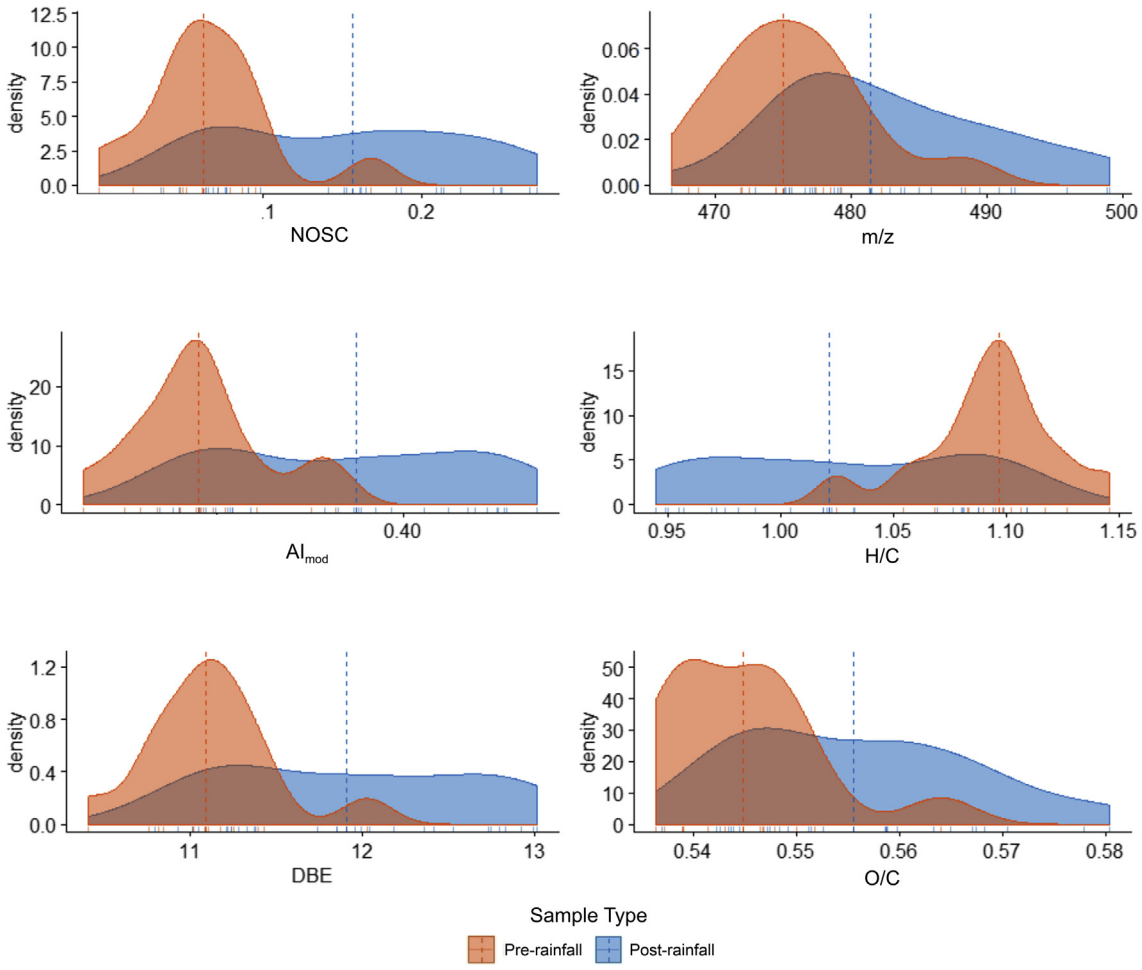

Fig. 3. Density curves for the weighted average nominal oxidation state of carbon (NOSC), mass to charge ratio (m/z), modified aromaticity index (AI_{mod}), hydrogen to carbon (H/C) ratio, double bond equivalent (DBE) and oxygen to carbon (O/C) ratio for pre-rainfall (n = 14) and post-rainfall (n = 28) samples. Red line indicates the median value for pre-rainfall samples. Blue dashed line indicates median for post-rainfall samples. (For interpretation of the references to colour in this figure legend, the reader is referred to the Web version of this article.)

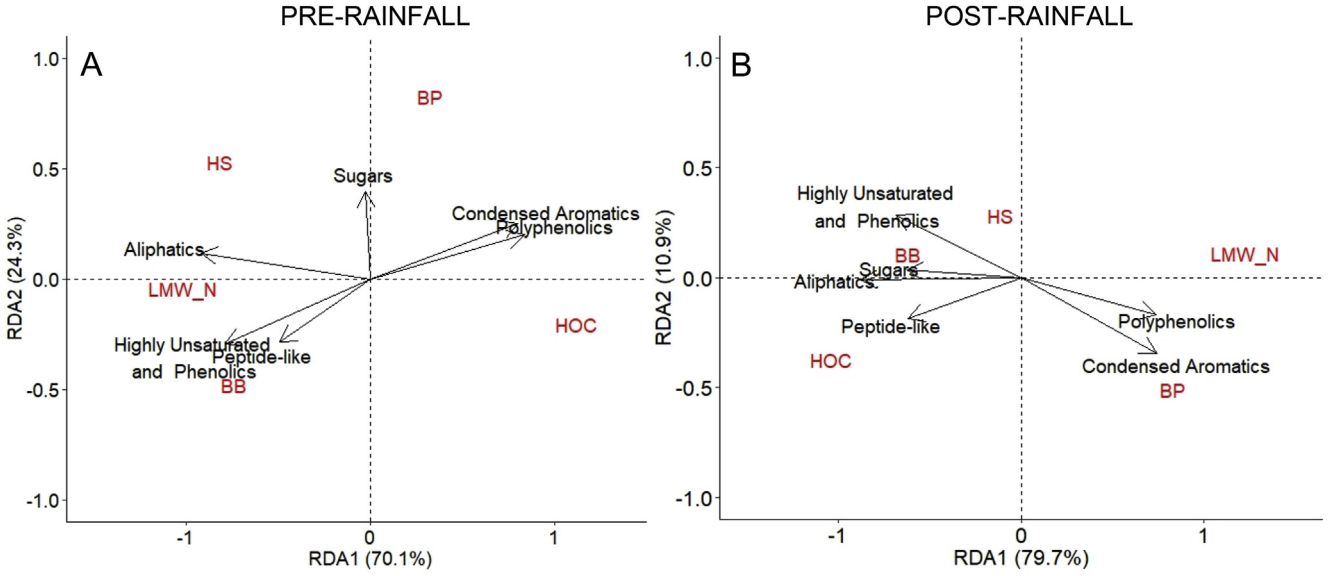

Fig. 4. Redundancy analysis showing HOC % RA is associated with different FT-ICR MS groups in pre- (A) and post-rainfall (B) samples on component 1, explaining 70.1% and 79.9% of the data respectively. Component 1 of the redundancy analysis on pre-rainfall samples shows HOC % RA is associated with polyphenolics % RA and condensed aromatics % RA. In post-rainfall samples HOC is most closely associated with aliphatics % RA and highly unsaturated and phenolics % RA (Table A.2). R code adapted from Hutchins et al. (2017).

models of post-rainfall data which show negative correlations between HOC % RA and polyphenolic % RA ($p = 1.17 \times 10^{-2}$) and % RA aromatics ($p = 9.78 \times 10^{-3}$), and positive correlations with % RA highly unsaturated and phenolics ($p = 2.05 \times 10^{-3}$) and % RA aliphatics ($p = 7.87 \times 10^{-4}$).

4. Discussion

Coastal peatlands are significant stores of carbon, however changes in precipitation regimes are likely to alter coastal peatland carbon dynamics and inorganic chemistry. Many people rely on coastal aquifers for fresh drinking water, domestic water supply, irrigation water and water for industry (Ferguson and Gleeson, 2012; Small and Nicholls, 2003). Water supply however can be impacted by high amounts of DOM and inorganic ions exported from these coastal peatlands, which subsequently requires removal via water treatment processes. The ease and cost of water treatment is largely dependent upon the character and the amount of DOM (Fabris et al., 2003) and inorganic contaminants present in source water. To date it has been unclear how changing precipitation regimes may affect the quality of groundwater in coastal peatlands.

Our results indicate that extreme rainfall events will cause the character of groundwater DOM in peat-rich sandy aquifers to shift to that of a more aromatic nature due to leaching from peat layers. This is probably attributed to physicochemical sorption equilibria mechanisms after dilution (Qualls and Richardson, 2003). The movement of water from the dunes to the wetland indicates that this highly aromatic DOM probably originates from peat leachate either from peat layers in the dune area or peat located in the shallow aquifer sampling area (Fig. 5). These findings indicate that prolonged drying events followed by extreme rainfall events expected in the future may flush previously stored aromatic DOM into groundwater where it is available to be processed or exported. In some MLS sample ports however, the amount of dilution appears to be restricted, suggesting that low permeability in some areas is limiting the exchange of water and solutes between peat pore water and rainfall recharge in these locations (Rezanezhad et al., 2016). The extent of aromatic DOM flushed into groundwater in peatlands after rainfall events therefore appears to be directly related to the permeability of the peat. This suggests that shallower, less compact peat layers may play a larger role in the flushing of aromatic DOM into groundwater.

As with aromaticity, the hydrophobicity of groundwater OM in peatland environments is also highly variable and impacted by changes in rainfall (Broder et al., 2017; Scott et al., 1998; Tang et al., 2013). RDA shows that HOC is associated with more aromatic groups pre-rainfall and less aromatic groups post-rainfall (Fig. 4, Table A.2). Linear modelling shows that in pre-rainfall samples HOC is positively correlated with NOSC. Compounds with high nominal oxidation state of carbon (NOSC) are more thermodynamically favourable to oxidise and thus associated with more bioavailable

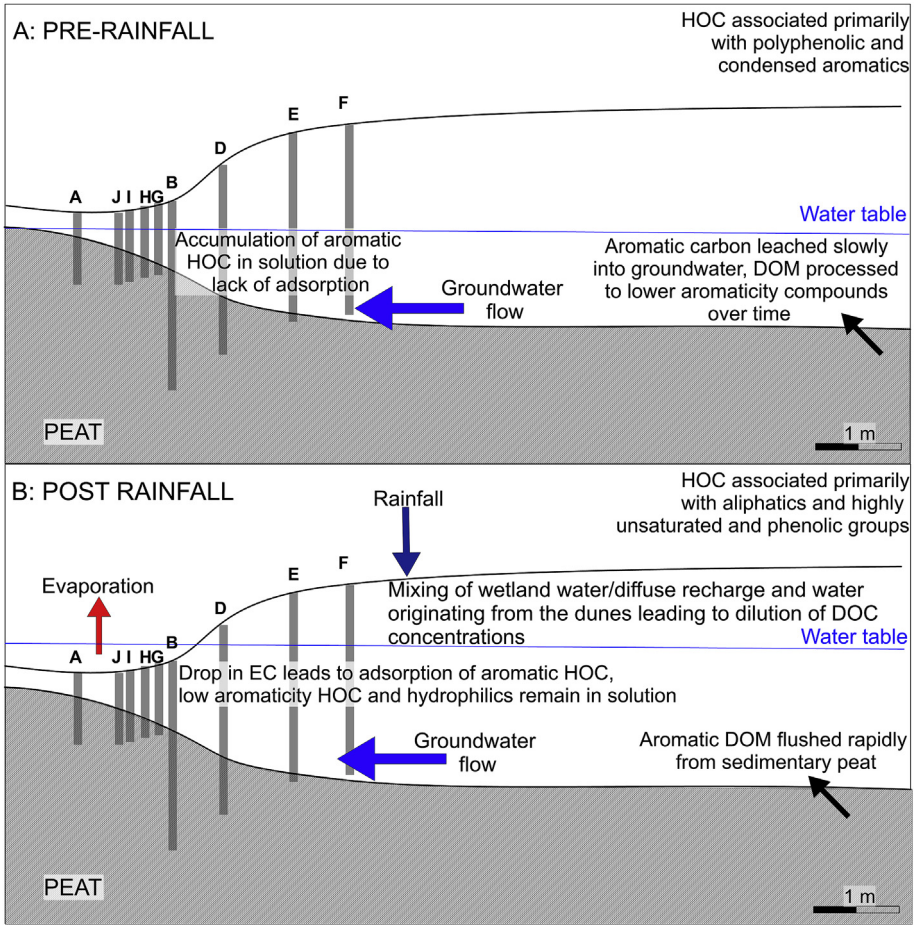

Fig. 5. Diagram of processes affecting DOM in the shallow aquifer of Anna Bay pre- and post-rainfall. Pre-rainfall, water comes from the wetland and dune areas, with aromatic DOM leached from peat and remaining in solution where it is broken down into smaller, more hydrophilic compounds. Post-rainfall a change in sorption equilibria due to fresh rainwater input causes an increase in the aromatic DOM leached from sedimentary peat. The hydrophobic portion of this DOM adsorbs to mineral surfaces leaving less aromatic hydrophobics in solution.

DOM (Keiluweit et al., 2016), particularly in environments low in energetic electron acceptors (i.e. oxygen and nitrate) such as Anna Bay (Table A.1). Research shows that aromatics with high NOSC are targeted first by microbes in anaerobic environments (Pracht et al., 2018). The positive correlation between HOC and NOSC, and the observation of high HOC, which the RDA shows is associated with aromatic unprocessed OM, indicates that HOC in pre-rainfall samples is likely the result of a steady accumulation of HOC sourced from buried peat that has evaded biodegradation (Fig. 5).

The observation of high HOC in pre-rainfall samples and declining HOC in post-rainfall samples contrasts with research which indicates that higher hydrophilic OC/HOC ratios should be observed in dry conditions due to the fact that hydrophilics desorb from mineral surfaces quickly compared to HOC (Scott et al., 1998; Tang et al., 2013). In high ionic strength solutions, research has shown that DOM forms coils that concentrate hydrophobic domains in the centre (Pedersen et al., 1999). This leads to less exposure of the hydrophobic adsorption points, which we propose results in the accumulation of the more aromatic HOC observed in the pre-rainfall RDA (Fig. 4). The decrease in ionic strength post-rainfall likely resulted in sorption of these aromatic hydrophobics (as indicated by the RDA) by causing the OM molecules to uncoil. Previous studies have also observed the preferential adsorption of higher molecular mass, more aromatic HOC (Filella, 2006; Jardine et al., 1989; Kaiser et al., 1996; Kaiser and Zech, 1997), particularly in high OC environments such as at Anna Bay.

Our results show significant increases in groundwater As post-rainfall. Previous research has shown that DOM can mobilise As from sediments due to competitive sorption (Bauer and Blodau, 2006). This mechanism is supported by a significant negative correlation between As and HOC in pre-rainfall samples ($p = 2.02 \times 10^{-2}$). The lack of correlation between As and HOC post-rainfall ($p = 7.68 \times 10^{-2}$) could be attributed to the almost complete removal of HOC from solution, and the flushing of desorbed As through the system during rainfall events. Other mechanisms for As release include pyrite oxidation and Fe-oxide dissolution, however we do not observe an increase in Fe in solution (Table 1) post-rainfall, there is no correlation observed between Fe and As observed pre- or post-rainfall, and there is no increase in SO_4 (Table 1) or decrease in pH ($p > 0.05$) which would be expected to be associated with pyrite oxidation (Appelo and Postma, 2005). Our results show a median As concentration increase of 47% post-rainfall, leading to concentrations greater than 3 times the World Health Organisation (WHO) guideline value of 10 μg / L for drinking water.

This research shows that extreme rainfall events may increase the export of inorganic and organic contaminants such as hydrophilic DOM and As from coastal peatland groundwaters. Heavy rainfall events following prolonged dry periods may result in the requirement for more rigorous water treatment to meet drinking water quality guidelines. Increased hydrophilic DOM in groundwater in high sedimentary OC environments will result in increasing difficulty to treat due to the low removal efficiency of hydrophilic DOM during water treatment processes (Alexander et al., 2012; Edzwald, 1993; Matilainen et al., 2010; Peter et al., 2019), and due to the increased formation potential of haloacetic acids (a harmful disinfectant by-product) during bio-treatment as a result of hydrophilic compounds (Bond et al., 2009). We note that as the changes observed appear to be largely driven by DOM sourced from sedimentary OC, these findings are likely specific to coastal wetland environments which exceed an area of 1.64×10^6 km^2 globally (Davidson and Finlayson, 2018). Further research would also benefit from an assessment of the changes to groundwater chemistry and DOM pre- and post-rainfall in low sedimentary OC coastal environments.

5. Conclusions

LC-OCD and FT-ICR MS techniques were used to investigate the changes to DOM character specifically associated with extreme rainfall events following drought conditions. The work highlights the benefit of using multiple DOM characterisation techniques to understand DOM character, sources and processing. The results show that DOM amount and character in coastal peatlands is highly dynamic and depends largely on hydrologic regimes, DOM sources and DOM processing mechanisms. This research confirms the hypothesis that rainfall events after dry conditions result in the leaching of sedimentary OC and changes the groundwater DOM character in these environments. The findings suggest that under the more extreme rainfall conditions anticipated in the future (Wasko and Sharma, 2017), leaching of peat after heavy rainfall events could increase As concentrations and change the character of DOM, increasing its hydrophilic/HOC ratio due to sorption of aromatic HOC. This will make groundwater in these areas more difficult and expensive to treat in the future (Alexander et al., 2012; Bond et al., 2009).

Author contributions

L.K.M. drafted the manuscript, performed data analysis and prepared figures and maps. A.B., M.S.A., D.M.O., H.R. and K.M. supervised the project and provided manuscript comments and guidance. C.B. and P.O. assisted with sample collection, data processing and data analysis. H.H. provided interpretations of sorption mechanisms related to LC-OCD data. C.M. provided guidance on manuscript direction and provided manuscript comments. M.I.B., R.G.M.S. and A.M. analysed samples for FT-ICR MS, provided text for Section 2.3 and manuscript comments.

Declaration of competing interest

The authors declare that they have no known competing financial interests or personal relationships that could have appeared to influence the work reported in this paper.

Acknowledgements

The authors would like to thank David Podgorski, Pheobe Zito, Khorshed Chinu and staff from the National High Magnetic Field Laboratory at Florida State University and the Mark Wainwright Analytical Centre at UNSW Sydney for the analysis of samples. The authors also thank Sabina Rakhimbekova for her assistance in sample collection.

This work was supported by the Australian Research Council [Discovery Project number DP160101379]; the Australian Government Research Training Program and Australian Nuclear Science Technology Organisation (ANSTO) for scholarship funding. This work was also made possible by grants from the Federal Government initiative National Collaborative Research Infrastructure Strategy (NCRIS), the NSW Department of Primary Industries Office of Water and the National Centre for Groundwater Research and Training (NCGRT). A portion of this work was performed at the National High Magnetic Field Laboratory ICR User Facility, which is supported by the National Science Foundation Division of Chemistry through DMR-1644779 and the State of Florida.

Appendix A. Supplementary data

Supplementary data to this article can be found online at https://doi.org/10.1016/j.watres.2019.115201.

References

Alexander, J.T., Hai, F.I., Al-aboud, T.M., 2012. Chemical coagulation-based processes for trace organic contaminant removal: current state and future potential. J. Environ. Manag. 111, 195–207.

Andersen, M.S., Castilla, J.C., Studholme, H., McCulloch, S., Acworth, I., 2012. Development of a Coastal Groundwater Process Investigation Site Anna Bay, New South Wales, Final Report Prepared for New South Wales Office of Water.

Appelo, C., Postma, D., 2005. Geochemistry, Groundwater and Pollution, second ed. CRC Press, Rotterdam (Balkema).

Bauer, M., Blodau, C., 2006. Mobilization of arsenic by dissolved organic matter from iron oxides, soils and sediments. Sci. Total Environ. 354, 179–190.

Bell, S.A.J., 1997. Tomaree National Park Vegetation Survey: A Fire Management Document East Coast Flora Survey, Report to the National Parks and Wildlife Service.

Bodmer, P., Heinz, M., Pusch, M., Singer, G., Premke, K., 2016. Carbon dynamics and their link to dissolved organic matter quality across contrasting stream ecosystems. Sci. Total Environ. 553, 574–586.

Boldin, I.A., Nikolaev, E.N., 2011. Fourier transform ion cyclotron resonance cell with dynamic harmonization of the electric field in the whole volume by shaping of the excitation and detection electrode assembly. Rapid Commun. Mass Spectrom. 25 (1), 122–126.

Bond, T., Goslan, E.H., Jefferson, B., Roddick, F., Fan, L., Parsons, S.A., 2009. Chemical and biological oxidation of NOM surrogates and effect on HAA formation. Water Res. 43 (10), 2615–2622.

Broder, T., Knorr, K.H., Biester, H., 2017. Changes in dissolved organic matter quality in a peatland and forest headwater stream as a function of seasonality and hydrologic conditions. Hydrol. Earth Syst. Sci. 21 (4), 2035–2051.

Brügger, C., 2018. Study of an Anoxic, Organic Matter Rich Groundwater System : Samurai Beach. UNSW Sydney and Université de Neuchâtel, New South Wales, Australia.

Chen, M., Kim, S., Park, J.-E., Jung, H.-J., Hur, J., 2016. Structural and compositional changes of dissolved organic matter upon solid-phase extraction tracked by multiple analytical tools. Anal. Bioanal. Chem. 408 (23), 6249–6258.

Chen, T., Beu, S.C., Kaiser, N.K., Hendrickson, C.L., 2014. Note: optimized circuit for excitation and detection with one pair of electrodes for improved Fourier transform ion cyclotron resonance mass spectrometry. Rev. Sci. Instrum. 85 (6), 0666107/0666101-0066107/0666103.

Corilo, Y., 2015. PetroOrg. The Florida State University, Tallahassee, FL.

Dalva, M., Moore, T., 1991. Sources and sinks of dissolved organic carbon in a forested swamp catchment. Biogeochemistry 15 (1), 1–19.

Davidson, N.C., Finlayson, C.M., 2018. Extent, regional distribution and changes in area of different classes of wetland. Mar. Freshw. Res. 69, 1525–1533.

Derrien, M., Brogi, S.R., Gonçalves-Araujo, R., 2019. Characterization of aquatic organic matter: assessment, perspectives and research priorities. Water Res. 163, 114908.

Dittmar, T., Koch, B., Herkorn, N., Kattner, G., et al., 2008. A simple and efficient method for the solid-phase extraction of dissolved organic matter (SPE-DOM) from seawater. Limnol Oceanogr. Methods 6 (6), 230–235. https://doi.org/10.4319/lom.2008.6.230.

Dulaquais, G., Breitenstein, J., Waeles, M., Marsac, R., Riso, R., 2018. Measuring dissolved organic matter in estuarine and marine waters: size-exclusion chromatography with various detection methods. Environ. Chem. 15 (7), 436–449.

Edzwald, J.K., 1993. Coagulation in drinking water treatment: particles, organics and coagulants. Water Sci. Technol. 27 (11), 21–35.

Emmett, M.R., White, F.M., Hendrickson, C.L., Shi, S.D.-H., Marshall, A.G., 1998. Application of micro-electrospray liquid chromatography techniques to FT-ICR MS to enable high-sensitivity biological analysis. J. Am. Soc. Mass Spectrom. 9 (4), 333–340.

Fabris, R., Chow, C., Drikas, M., 2003. Natural Organic Matter in Drinking Water: Problems & Solution. Cooperative Research Centre for Water Quality and Treatment Salisbury, South Australia.

Ferguson, G., Gleeson, T., 2012. Vulnerability of coastal aquifers to groundwater use and climate change. Nat. Clim. Chang. 2, 342.

Filella, M., 2006. Colloidal properties of submicron particles in natural waters. Environ.Colloids. Part. 10, 17–93.

Guppy, C.N., Menzies, N.W., Moody, P.W., Blamey, F.P.C., 2005. Competitive sorption reactions between phosphorus and organic matter in soil: a review. Aust. J. Soil Res. 43, 189–202.

Harvey, C.F., Swartz, C.H., Badruzzaman, A.B.M., Keon-Blute, N., Yu, W., Ali, M.A., Jay, J., Beckie, R., Niedan, V., Brabander, D., Oates, P.M., Ashfaque, K.N., Islam, S., Hemond, H.F., Ahmed, M.F., 2002. Arsenic mobility and groundwater extraction in Bangladesh. Science 298 (5598), 1602.

He, W., Chen, M., Park, J.-E., Hur, J., 2016. Molecular diversity of riverine alkaline-extractable sediment organic matter and its linkages with spectral indicators and molecular size distributions. Water Res. 100, 222–231.

Hendrickson, C.L., Quinn, J.P., Kaiser, N.K., Smith, D.F., Blakney, G.T., Chen, T., Marshall, A.G., Weisbrod, C.R., Beu, S.C., 2015. 21 Tesla Fourier transform ion cyclotron resonance mass spectrometer: a national resource for ultrahigh resolution mass analysis. J. Am. Soc. Mass Spectrom. 26, 1626–1632.

Huber, S.A., Balz, A., Abert, M., Pronk, W., 2011. Characterisation of aquatic humic and non-humic matter with size-exclusion chromatography – organic carbon detection – organic nitrogen detection (LC-OCD-OND). Water Res. 45 (2), 879–885.

Hutchins, R.H.S., Aukes, P., Schiff, S.L., Dittmar, T., Prairie, Y.T., del Giorgio, P.A., 2017. The optical, chemical, and molecular dissolved organic matter succession along a boreal soil-stream-river continuum. J. Geophys. Res.: Biogeosciences 122 (11), 2892–2908.

Jardine, P.M., McCarthy, J.F., Weber, N.L., 1989. Mechanisms of dissolved organic carbon adsorption on soil. Soil Sci. Soc. Am. J. 53 (5), 1378–1385.

Jung, C., Deng, Y., Zhao, R., Torrens, K., 2017. Chemical oxidation for mitigation of UV-quenching substances (UVQS) from municipal landfill leachate: fenton process versus ozonation. Water Res. 108, 260–270.

Kaiser, K., Guggenberger, G., Zech, W., 1996. Sorption of DOM and DOM fractions to forest soils. Geoderma 74 (3), 281–303.

Kaiser, K., Zech, W., 1997. Competitive sorption of dissolved organic matter fractions to soils and related mineral phases. Soil Sci. Soc. Am. J. 61 (1), 64–69.

Kaiser, N.K., Savory, J.J., Hendrickson, C.L., 2014. Controlled ion ejection from an external trap for extended *m/z* range in FT-ICR mass spectrometry. J. Am. Soc. Mass Spectrom. 25, 943–949.

Keiluweit, M., Nico, P.S., Kleber, M., Fendorf, S., 2016. Are oxygen limitations under recognized regulators of organic carbon turnover in upland soils? Biogeochemistry 127 (2), 157–171.

Koch, B.P., Dittmar, T., 2006. From mass to structure: an aromaticity index for high-resolution mass data of natural organic matter. Rapid Commun. Mass Spectrom. 20 (5), 926–932.

Koch, B.P., Dittmar, T., Witt, M., Kattner, G., 2007. Fundamentals of molecular formula assignment to ultrahigh resolution mass data of natural organic matter. Anal. Chem. 79 (4), 1758–1763.

Lalonde, K., Mucci, A., Ouellet, A., Gélinas, Y., 2012. Preservation of organic matter in sediments promoted by iron. Nature 483, 198.

Leng, L.Y., Ahmed, O.H., Jalloh, M.B., 2019. Brief review on climate change and tropical peatlands. Geosci. Front. 10 (2), 373–380.

Lipczynska-Kochany, E., 2018. Effect of climate change on humic substances and associated impacts on the quality of surface water and groundwater: a review. Sci. Total Environ. 640–641, 1548–1565.

Lis, G., Wassenaar, L.I., Hendry, M.J., 2008. High-precision laser spectroscopy D/H and 18O/16O measurements of microliter natural water samples. Anal. Chem. 80 (1), 287–293.

Luzius, C., Guillemette, F., Podgorski, D.C., Kellerman, A.M., Spencer, R.G.M., 2018. Drivers of dissolved organic matter in the vent and major conduits of the world's largest freshwater spring. J. Geophys. Res.: Biogeosciences 123 (9), 2775–2790.

Maier, R.M., 2015. Biogeochemical cycling. In: Pepper, I.L., Gerba, C.P., Gentry, T.J. (Eds.), Environmental Microbiology, third ed. Academic Press, San Diego, pp. 339–373.

Matilainen, A., Vepsäläinen, M., Sillanpää, M., 2010. Natural organic matter removal by coagulation during drinking water treatment: a review. Adv. Colloid Interface Sci. 159 (2), 189–197.

Meredith, K.T., Baker, A., Andersen, M.S., O'Carroll, D.M., Rutlidge, H., McDonough, L.K., Oudone, P., Bryan, E., Zainuddin, N.S., 2019. Isotopic and chromatographic fingerprinting of the sources of dissolved organic carbon in a shallow coastal aquifer. Hydrol. Earth Syst. Sci. Discuss. 1–20, 2019.

Pedersen, J.A., Gabelich, C.J., Lin, C.-H., Suffet, I.H., 1999. Aeration effects on the partitioning of a PCB to anoxic estuarine sediment pore water dissolved organic matter. Environ. Sci. Technol. 33 (9), 1388–1397.

Peter, K.T., Herzog, S., Tian, Z., Wu, C., McCray, J.E., Lynch, K., Kolodziej, E.P., 2019. Evaluating emerging organic contaminant removal in an engineered hyporheic zone using high resolution mass spectrometry. Water Res. 150, 140–152.

Post, V.E.A., 2005. Fresh and saline groundwater interaction in coastal aquifers: is our technology ready for the problems ahead? Hydrogeol. J. 13 (1), 120–123.

Pracht, L.E., Tfaily, M.M., Ardissono, R.J., Neumann, R.B., 2018. Molecular characterization of organic matter mobilized from Bangladeshi aquifer sediment: tracking carbon compositional change during microbial utilization. Biogeosciences 15 (6), 1733–1747.

Qualls, R., Richardson, C., 2003. Factors controlling concentration, export, and decomposition of dissolved organic nutrients in the Everglades of Florida. Biogeochemistry 62 (2), 197–229.

Rakhimbekova, S., O'Carroll, D.M., Andersen, M.S., Wu, M.Z., Robinson, C.E., 2018. Effect of transient wave forcing on the behavior of arsenic in a nearshore aquifer. Environ. Sci. Technol. 52 (21), 12338–12348.

Retelletti Brogi, S., Ha, S.-Y., Kim, K., Derrien, M., Lee, Y.K., Hur, J., 2018. Optical and molecular characterization of dissolved organic matter (DOM) in the Arctic ice core and the underlying seawater (Cambridge Bay, Canada): implication for increased autochthonous DOM during ice melting. Sci. Total Environ. 627, 802–811.

Rezanezhad, F., Price, J.S., Quinton, W.L., Lennartz, B., Milojevic, T., Van Cappellen, P., 2016. Structure of peat soils and implications for water storage, flow and solute transport: a review update for geochemists. Chem. Geol. 429, 75–84.

Rieley, J.O., Wüst, R.A.J., Jauhiainen, J., Page, S.E., Wösten, J.H.M., Hooijer, A., Siegert, E., Limin, S.H., Vasander, H., Stahlhut, M., 2008. In: Strack, M. (Ed.), Peatlands and Climate Change. International Peat Society, Jyväskylä, pp. 148–181.

Rogers, K., Kelleway, J.J., Saintilan, N., Megonigal, J.P., Adams, J.B., Holmquist, J.R., Lu, M., Schile-Beers, L., Zawadzki, A., Mazumder, D., Woodroffe, C.D., 2019. Wetland carbon storage controlled by millennial-scale variation in relative sea-level rise. Nature 567 (7746), 91–95.

Savory, J.J., Kaiser, N.K., McKenna, A.M., Xian, F., Blakney, G.T., Rodgers, R.P., Hendrickson, C.L., Marshall, A.G., 2011. Parts-Per-Billion Fourier transform ion

cyclotron resonance mass measurement accuracy with a "Walking" calibration equation. Anal. Chem. 83 (5), 1732–1736.
Scott, M.J., Jones, M.N., Woof, C., Tipping, E., 1998. Concentrations and fluxes of dissolved organic carbon in drainage water from an upland peat system. Environ. Int. 24 (5), 537–546.
Small, C., Nicholls, R.J., 2003. A global analysis of human settlement in coastal zones. J. Coast. Res. 19 (3), 584–599.
Smith, D.F., Podgorski, D.C., Rodgers, R.P., Blakney, G.T., Hendrickson, C.L., 2018. 21 Tesla FT-ICR mass spectrometer for ultrahigh resolution analysis of complex organic mixtures. Anal. Chem. 90 (3), 2041–2047.
Tang, R., Clark, J.M., Bond, T., Graham, N., Hughes, D., Freeman, C., 2013. Assessment of potential climate change impacts on peatland dissolved organic carbon release and drinking water treatment from laboratory experiments. Environ. Pollut. 173, 270–277.
Thomas, J.C., Lutz, M.A., Bruce, J.L., Graczyk, D.J., Richards, K.D., Krabbenhoft, D.P., Westenbroek, S.M., Scudder, B.C., Sullivan, D.J., Bell, A.H., 2007. Water-Quality Characteristics for Selected Sites within the Milwaukee Metropolitan Sewerage District Planning Area. Wisconsin, February 2004-September 2005.
Wang, S., Zhuang, Q., Lähteenoja, O., Draper, F.C., Cadillo-Quiroz, H., 2018. Potential shift from a carbon sink to a source in Amazonian peatlands under a changing climate. Proc. Natl. Acad. Sci. 115 (49), 12407.
Wasko, C., Sharma, A., 2017. Continuous rainfall generation for a warmer climate using observed temperature sensitivities. J. Hydrol. 544, 575–590.
Xu, J., Morris, P.J., Liu, J., Holden, J., 2018. PEATMAP: refining estimates of global peatland distribution based on a meta-analysis. Catena 160, 134–140.